Title
Communication of Ca2+ signals via tunneling membrane nanotubes is mediated by transmission of inositol trisphosphate through gap junctions

Journal
Cell Calcium, 60(4)

ISSN
0143-4160

Authors
Lock, Jeffrey T
Parker, Ian
Smith, Ian F

Publication Date
2016-10-01

DOI
10.1016/j.ceca.2016.06.004

Peer reviewed

HHS Public Access

Author manuscript

Cell Calcium. Author manuscript; available in PMC 2017 October 01.

Published in final edited form as:

Cell Calcium. 2016 October ; 60(4): 266–272. doi:10.1016/j.ceca.2016.06.004.

Communication of Ca^{2+} signals via tunneling membrane nanotubes is mediated by transmission of inositol trisphosphate through gap junctions

Jeffrey T. Lock[a], **Ian Parker**[a,b], and **Ian F. Smith**[a]

Jeffrey T. Lock: lockj@uci.edu; Ian Parker: iparker@uci.edu; Ian F. Smith: ismith@uci.edu

[a]Department of Neurobiology and Behavior, University of California, Irvine, CA

[b]Department of Physiology and Biophysics, University of California, Irvine, CA

Abstract

Tunneling membrane nanotubes (TNTs) are thin membrane projections linking cell bodies separated by many micrometers, which are proposed to mediate signaling and even transfer of cytosolic contents between distant cells. Several reports describe propagation of Ca^{2+} signals between distant cells via TNTs, but the underlying mechanisms remain poorly understood. Utilizing a HeLa M-Sec cell line engineered to upregulate TNTs we replicated previous findings that mechanical stimulation elicits robust cytosolic Ca^{2+} elevations that propagate to surrounding, physically separate cells. However, whereas this was previously interpreted to involve intercellular communication through TNTs, we found that Ca^{2+} signal propagation was abolished - even in TNT-connected cells - after blocking ATP-mediated paracrine signaling with a cocktail of extracellular inhibitors. To then establish whether gap junctions may enable cell-cell signaling via TNTs under these conditions, we expressed sfGFP-tagged connexin-43 (Cx43) in HeLa M-Sec cells. We observed robust communication of mechanically-evoked Ca^{2+} signals between distant but TNT-connected cells, but only when both cells expressed Cx43. Moreover, we also observed communication of Ca^{2+} signals evoked in one cell by local photorelease of inositol 1,4,5-trisphosphate (IP_3). Ca^{2+} responses in connected cells began after long latencies at intracellular sites several microns from the TNT connection site, implicating intercellular transfer of IP_3 and subsequent IP_3-mediated Ca^{2+} liberation, and not Ca^{2+} itself, as the mediator between TNT-connected, Cx43-expressing cells. Our results emphasize the need to control for paracrine transmission in studies of cell-cell signaling via TNTs and indicate that, in this cell line, TNTs do not establish cytosolic continuity between connected cells but rather point to the crucial importance of connexins to enable communication of cytosolic Ca^{2+} signals via TNTs.

Corresponding author: Ian F. Smith, ismith@uci.edu.

Disclosures

All authors declare they have no competing financial interests.

Author contributions

Conception and design of the study by J.T.L, I.F.S, and I.P. Data was collected by J.T.L and analyzed by J.T.L, I.P, and I.F.S. Manuscript was written by J.T.L, I.F.S and I.P. All authors have read and approve the published manuscript.

Graphical Abstract

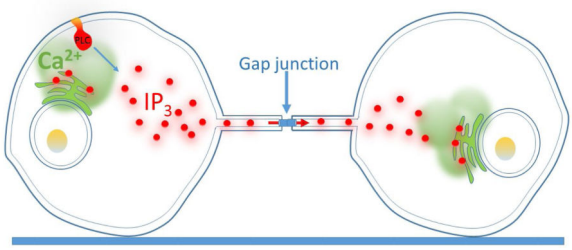

Keywords

Tunneling nanotubes; TNTs; Ca^{2+} signaling; Connexin 43; IP_3; paracrine signaling

1. Introduction

Intercellular communication is vital to co-ordinate the proper functioning of tissues and organs, and cells have long been known to employ gap junctions and synapses to achieve this function. In 2004 a new route of cell-to-cell communication was proposed based on the discovery of tunnelling membrane nanotubes (TNTs) [1]. TNTs are membrane protrusions, a few to several hundred nanometers in diameter that physically link distinct cell bodies over many micrometers. TNT-like structures have been found in numerous mammalian cells, including cultured cell lines such as THP-1 monocytes [2], Raw264.6 macrophages [3], ARPE-19 retinal pigment epithelial cells [4], human neuroblastoma SH-SY5Y cells [5], human breast cancer MCF-7 cells [6]; as well as in isolated primary cells such as human monocyte derived dendritic cells [2], neonatal neurons and astrocytes [7], neonatal rat cardiomyocytes and fibroblasts [8], human T cells [9]; and between cells in intact tissues, including dendritic cells in the corneal stroma [10] and astrocytoma cells in the mouse brain [11]. Several distinct and diverse cellular functions have been proposed for TNTs, including intercellular transfer of mitochondria and organelles [1, 12, 13]; transfer of virus [9, 14] and prion proteins [15]; and intercellular exchange of Ca^{2+} signals [2–5, 7, 8, 11, 16, 17].

The spatial and temporal patterning of cytosolic Ca^{2+} signals tightly regulate a panoply of biological functions [18]. Communication of Ca^{2+} signals via TNTs provides a cellular level of specificity that contrasts with the promiscuous nature of paracrine-mediated Ca^{2+} signaling, and extends the range of communication so that cells do not need to be physically abutted as in classical gap junction-mediated signaling [19]. Such long-range Ca^{2+} signaling between distant cells may be involved in coordination within tissues to control physiological functions as varied as gene expression, secretion and synaptic plasticity [20], and in the pathophysiology of diverse diseases including Alzheimer's, cardiac arrhythmias and cancer [9, 11, 15, 21]. Notably, a recent report describes that TNTs establish a Ca^{2+} signaling network in astrocytoma cells and that disruption of this network by knockdown of connexin 43 results in a reduction of tumor size [11].

In this report we demonstrate that intercellular Ca^{2+} wave propagation between distant cells via membrane nanotubes requires cells to be functionally coupled by gap junctions. We

further show that diffusion of IP_3 and not Ca^{2+} is responsible for propagating a regenerative Ca^{2+} signal.

2. Experimental methods

2.1 Cell Culture

HeLa cells stably expressing M-Sec vector were a gift from Hiroshi Ohno (Riken Institute, Japan). HeLa-M-Sec cells were maintained at 37°C in humidified environment with 95% air and 5% CO_2 in DMEM (Thermofisher; #11965) supplemented with 10% FBS (Omega Scientific, # FBS-11(lot#593515)) and 100 μg/ml G418 (Thermofisher; #10131035). For experimentation, cells were harvested by incubation with 0.25% Trypsin-EDTA (Gibco; #25200-056) and sub-cultured (50,000 cells per ml) on 35 mm glass-bottom imaging dishes (MatTek; #P35-1.5-14-C) for 1–3 days prior to imaging.

For experiments requiring expression of connexin-43 (Cx43; kindly provided by David Spray, Albert Einstein College of Medicine, USA), 10^6 cells were electroporated (Neon transfection system; Invitrogen) with 5 μg of Cx43 tagged with superfolder-GFP (sfGFP) to its amino-terminus (Cx43-sfGFP) and sub-cultured at two different densities (50,000 and 25,000 cells per ml) in 35 mm imaging dishes. Cells transfected with Cx43-sfGFP were used between 24–48 hours.

2.2 Material and reagents

The acetoxymethyl (AM) ester forms of the organic Ca^{2+}-dyes Cal-520 and Cal-590 (AAT Bioquest #21130 and #20511, respectively) were reconstituted with dimethyl sulfoxide (DMSO) containing 20% pluronic F-127 (DMSO/F-127; Invitrogen; #P-3000MP) to a final concentration of 1 mM and were stored, shielded from light, at -20°C. The membrane-permeant caged IP_3 analogue ci-IP_3/PM (D-2,3-O-Isopropylidene-6-O-[2-nitro-4,5 dimethoxy] benzyl-myo-Inositol 1,4,5-trisphosphate Hexakis [propionoxymethyl] ester) was purchased from siChem (#cag-iso-2-145-10), solubilized with DMSO/F-127 (Thermofisher; #P300MP) to a final concentration of 400 μM and stored at -20°C. Apyrase (#A6410) and suramin (#S2671) from Sigma-Aldrich were, respectively, prepared to 1 unit per μl and 50 mM using deionized-H_2O (di-H_2O) and stored at -50°C. The caged ATP analogue (adenosine 5'-triphosphate, P^3-[1-[2-nitrophenyl]ethyl] ester, disodium salt) was purchased from Invitrogen (#A-1048), solubilized to 50 mM with di-H_2O and stored, shielded from light, at -20°C. Deep Red plasma membrane stain was purchased from Invitrogen (#C10046) and stored at -20°C. All other reagents were purchased from Sigma-Aldrich.

2.3 Ca^{2+} Imaging

Cell culture medium was replaced with a Ca^{2+}-containing HEPES buffered salt solution (Ca^{2+}-HBSS) composed of (mM): 135 NaCl, 5.4 KCl, 2 $CaCl_2$, 1 $MgCl_2$, 10 HEPES, and 10 glucose; pH=7.4 set with NaOH at room temperature (RT). Cells were then incubated with 5 μM of either Cal-520/AM or Cal-590/AM for one hour in Ca^{2+}-HBSS at RT. For experiments utilizing ci-IP_3 cells were loaded with 2 μM ci-IP_3 in conjunction with 5 μM Cal-520/AM or Cal-590/AM for 1 hr. Following loading, cells were washed with Ca^{2+}-HBSS for 30 min and then incubated with Deep Red plasma membrane stain, diluted

(1:5000) in Ca^{2+}-HBSS, for 10 minutes. Cells were then rinsed three times with Ca^{2+}-HBSS and immediately used for experimentation.

Imaging of cytosolic Ca^{2+} signals was accomplished using a home-built microscope system based around an Olympus IX 50 microscope equipped with an Olympus 100X objective (NA 1.40) described previously [22, 23]. Excitation light from the expanded beam of either 488 nm (Coherent, Santa Clara, CA), 532 nm (Coherent, Santa Clara, CA) or 561 nm (Opto-Engine, Midvale, UT) diode pumped solid-state (DPSS) lasers was introduced by a small reflective prism and brought to a focus at the rear focal plane of the objective. The laser spot was positioned near the center of the objective aperture to create wide-field (WF) excitation. Emitted fluorescence was collected through the same objective and filtered by steep-cut long pass filters (Semrock, Rochster, NY) with cut-off wavelengths corresponding to the respective laser wavelengths. Images were acquired by an Evolve 512 electron-multiplied c.c.d. camera (Photometrics, Tucson, AZ) with 512×512 pixel resolution (1 pixel = 0.166 μm) at a rate of 10 frames per sec (fps). Image data were streamed to computer memory using MetaMorph software (Universal Imaging/Molecular Devices, Sunnyvale, CA) and were subsequently stored on hard disc for offline analysis.

2.4 Mechanical stimulation and photorelease of ATP and i-IP_3

Mechanical stimulation (MS) was applied by gentle depression of the plasma membrane with a glass needle manually controlled by a hydraulic micromanipulator. Needles were fabricated from borosilicate glass capillary filaments (1.5mm×0.86mm; O.D.×I.D.) using a micro-pipet puller (Narishige, Japan) to produce tip diameters of ~1–2 micrometers. Dim transmitted light was used to guide the micropipette allowing the location and the strength of MS to be visually controlled during Ca^{2+} imaging experiments. To photo-release release caged-ATP, UV light, obtained from a xenon arc illuminator and filtered through a 350–400 nm bandpass, was introduced by a UV-reflecting dichroic in the light path uniformly focused throughout the field; the amount of caged-ATP released was controlled by varying the flash duration, set by an electronically controlled shutter (UniBlitz, Rochseter, NY). Spot UV photolysis of ci-IP_3 was achieved using a 405 nm laser (CivilLaser, Hangzhou, China) and galvanometer-driven mirrors interfaced with a custom-written algorithm to control the position and duration of the laser spot in order to selectively stimulate a single cell without the spurious activation of surrounding cells.

2.5 Image analysis

Image data in MetaMorph stk format were processed using a custom algorithm, written in the Python programming language, for the detection and analysis of whole-cell Ca^{2+} signals from fluorescence video recordings [24]. Image stacks were processed by first subtracting the background fluorescence from the entire image stack and then normalized by dividing the stack by the mean fluorescence of each pixel averaged over 100 frames prior to stimulation (F_0). Individual cells were manually identified and a region of interest (ROI), outlining the entire cell, was generated for all cells in the imaging field. Normalized fluorescence values from ROIs, corresponding to individual cells, was used to calculate amplitude and lag time of the Ca^{2+} response. Peak amplitude was measured as the change in fluorescence from baseline immediately preceding the event to the maximum fluorescence

value of the Ca^{2+} response. Lag time was quantified as the duration of time between the peak amplitude of the Ca^{2+} response in the stimulated cell to the peak response in the connected cell. Linescan kymograph images were derived by measuring fluorescence across a single line (width 6 pixels, 1 μm) from $\Delta F/F_0$ image stacks (created as described above), displaying their evolution over time as a pseudocolored representation utilizing the kymograph function in MetaMorph. Data are presented as mean ± sem.

3. Results

3.1 Transmission of Ca^{2+} signals between HeLa M-Sec cells

The mechanisms underlying Ca^{2+} signal transmission via TNTs remain poorly understood. To investigate this process we utilized HeLa cells stably expressing the M-Sec protein (also known as TNFaip2), which induces *de novo* formation of numerous TNTs between cells (>10 per cell pair) [3]. We visualized TNTs in HeLa M-Sec cultures using a Deep Red plasma membrane stain, observing fine 'finger-like' projections between cells (Figs. 1A,B; left panels) which, distinctive of TNTs, were located a few micrometers above the coverglass rather than adhering to the substrate [1]. Following procedures of a previous study describing cell-cell propagation of Ca^{2+} signals in >70% of TNT-connected HeLa M-Sec cell pairs following mechanical stimulation [3], we loaded these cells with the fluorescent Ca^{2+} indicator Cal-520 and mechanically stimulated a single cell by gentle touch with a micropipette to evoke a rapid rise in intracellular Ca^{2+} in that cell. In initial experiments we found that, in agreement with the earlier study [3] this local stimulation frequently gave rise to robust Ca^{2+} signals in TNT-connected cells (Figs.1a,c: 50%, 17 of 34 cells).

However, we also observed communication of Ca^{2+} signals to surrounding cells that were not connected by TNTs (37%; 20 of 53 cells). We thus became concerned that our attempts to study TNT-mediated transmission were being confounded by paracrine signaling, given that HeLa cells release ATP with mechanical stimulation [19] and express metabotropic purinergic receptors that couple to the IP_3/Ca^{2+} signaling pathway. Consistent with this notion, photorelease of ATP from a caged precursor in the bathing medium evoked strong Ca^{2+} signals, which we were able to effectively block only by incubating cells with a cocktail containing both apyrase (20 units/ml) and suramin (100 μM) (Supplementary Fig. S1). When incubated in this cocktail, mechanical stimulation still elicited rapid increases in Ca^{2+} in the stimulated cell (Fig. 1B), with amplitudes comparable to that seen without ATP signaling blockers (Figs. 1,D, E: 10.09 ± 0.66 $\Delta F/F_0$ vs 10.04 ± 0.68 for control cells), but responses in all surrounding cells, whether TNT-connected (n=28, Figs. 1B-F) or not (n=40) were completely abolished. We therefore performed all subsequent experiments involving mechanical stimulation in the presence of the ATP-blocking cocktail.

3.2 Role of gap junctions in signal propagation via TNTs

Gap junctions have recently been implicated in transmission of signaling molecules between TNT-connected cells, with endogenous connexins shown to localize in or near TNTs by immunofluoresence [4, 7, 17]. To then examine whether gap junctions could establish Ca^{2+} signal propagation between TNT-connected cells, we transiently expressed connexin 43 [25]

tagged with superfolded GFP (Cx43-sfGFP) in HeLa M-Sec cells and mechanically stimulated individual cells as before. For Ca^{2+} imaging we now used the red-shifted Ca^{2+} indicator Cal-590 to achieve spectral separation between sfGFP and Ca^{2+} images. Naïve HeLa cells are not coupled by gap junctions, but become able to transmit intercellular Ca^{2+} waves following expression of connexin [19]. We first confirmed the formation of functional gap junctions between directly abutted cells which both expressed Cx43-sfGFP. Mechanical stimulation of one cell evoked a rapid rise in intracellular Ca^{2+} that, after a short delay, produced a Ca^{2+} rise in abutting cells (8 of 11 trials, Supplementary Fig. S2). No transmission of Ca^{2+} signal was seen when one (n = 6 trials) or both (n = 5 trials) abutting cells failed to express Cx43-sfGFP.

Next, we identified pairs of cells that were clearly separated from one another but were connected by TNTs (Fig. 2A) and both expressed Cx43-sfGFP with fluorescent punctae visible at the base of TNTs or within the TNTs themselves (Fig. 2B). In the continued presence of suramin plus apyrase, mechanical stimulation of one cell evoked robust Ca^{2+} responses in the connected cell in 6 of 13 trials (Figs. 2C,D). The mean amplitude of Ca^{2+} signals in responding cells was smaller than in the stimulated cell (0.69 ± 0.1 $\Delta F/F_0$ *vs.* 1.99 ± 0.2 Figs. 2D,E), and maximal signals in responding cells occurred with a mean lag time of 9.6 ± 2.25 sec following the peak response in the stimulated cell. This delay was about 60% longer than observed in directly abutting, Cx43-expressing cells (6.01 ± 0.57 sec, n = 8), consistent with a greater distance and diffusional barriers for transmission of signaling molecules

3.3 Signal propagation via diffusion of IP_3 along TNTs

In addition to promoting the release of ATP, mechanical stimulation also stimulates the production of IP_3 and the subsequent release of Ca^{2+} from the ER through IP_3 receptor (IP_3R) channels [19]. To specifically address the role of the IP_3/Ca^{2+} pathway in communicating Ca^{2+} signals via TNTs we utilized local UV laser spot photolysis to photorelease i-IP_3 from a caged precursor in selected cells. In naïve HeLa M-Sec cells (i.e. not expressing connexins; Fig. 3A), UV spot uncaging of ci-IP_3 evoked robust Ca^{2+} signals in the stimulated cell ($\Delta F/F_0$ 4.26 ± 0.57, n=6 trials), but we never observed Ca^{2+} signals in surrounding cells whether TNT-connected (n=16 cells from 6 trials, Figs. 3B,C) or not (n = 15 cells from 6 trials). However, in pairs of TNT-connected cells where both expressed Cx43-sfGFP at the base of the TNT or within the TNT itself (Figs. 3D,E), i-IP_3-evoked Ca^{2+} signals in stimulated cells (Figs. 3F,G; mean peak $\Delta F/F_0$ 1.48 ± 0.12) were followed by delayed Ca^{2+} responses in 9 of 21 (43%) connected cells (Figs. 3F-H, mean peak $\Delta F/F_0$ 0.9 ± 0.13 in responding cells). The rise in Ca^{2+} in connected cells occurred with highly variable latencies following that in the i-IP_3-stimulated cell (mean 69.4 ± 14.8 s); appreciably longer than following mechanical stimulation (9.6 ± 2.2 sec).

In principle, propagation of a Ca^{2+} signal via TNTs might result from direct transfer of Ca^{2+}; from diffusion of IP_3 from the stimulated cell to evoke Ca^{2+} liberation in the responding cell; or from a mixed mechanism by which Ca^{2+} transfer potentiates IP_3-induced Ca^{2+} liberation in the responding cell[23]. To discriminate between these hypotheses we examined communication between TNT-connected, Cx43-expressing cell pairs (Figs. 4A,C)

by forming kymograph images of Ca^{2+} fluorescence to visualize the locations and timing of cytosolic Ca^{2+} elevations along lines drawn to connect both cells along the TNTs (Figs. 4B,C). As illustrated in Figs. 4B,D, respectively using mechanical stimulation and local photorelease of i-IP_3 as stimuli, a key finding was that Ca^{2+} elevations in responding cells began after appreciable delays (~ 5s for touch and ~35s for i-IP_3) at locations distant from the sites of TNT contact and without any perceptible preceding rise in Ca^{2+} within the TNT. Fig. 4E summarizes data from experiments with mechanical stimulation (6 cells) and photoreleased i-IP_3 (9 cells) response latencies and initial locations of Ca^{2+} responses in responding cells. Ca^{2+} responses began in responding cells at similar distances from the site of TNT contacts with both mechanical stimuli and photoreleased i-IP_3; shorter latencies were observed with mechanical stimuli, likely because mechanical stimulation produced more IP_3.

4. Discussion

The mechanism underlying transfer of Ca^{2+} signals between distant cells via TNTs following mechanical stimulation has variously been suggested to involve direct cytosolic [2, 4, 8, 11, 16] or membrane [3] continuity established by TNTs; or by transmission of depolarizing electrical signals between cells [7, 17]. Here, we used a HeLa M-Sec cell line that upregulates TNT formation [3]. After controlling for paracrine signaling (a well-established phenomenon in HeLa cells [19]) using a cocktail of purinergic signaling inhibitors, we found no evidence for transmission of Ca^{2+} signals in naïve cells that did not express connexins, in contrast to published findings [3]. We thus conclude that TNTs do not establish direct cytosolic continuity in this cell type. Discrepant findings regarding cytosolic continuity through TNTs may, in part, reflect their diverse morphological and functional properties across different cell types [26]; but we further caution the need to rigorously exclude paracrine mechanisms in studies of TNT signaling, a factor that may explain the previous description of TNT-mediated Ca^{2+} signal transmission in naïve HeLa M-Sec cells [3]. Rather, we found that expression of connexins within both paired TNT-coupled cells was an absolute requirement for the transmission of Ca^{2+} signals by TNTs. This transmission is unlikely to be mediated electrically [7, 17], as we failed to observe Ca^{2+} signals evoked by depolarization with 50 mM K^+ (n = 49 cells), and HeLa cell are not reported to express endogenous voltage gated Ca^{2+} channel. Moreover, we did not detect Ca^{2+} from a stimulated cell transiting through TNTs and into surrounding connected cells; a finding consistent with our previous modeling studies suggesting that TNTs are inefficient conduits for buffered diffusion of Ca^{2+} [5]. Instead, we propose that long distance cell-cell communication of Ca^{2+} signals is achieved by diffusion of IP_3 along gap junction-coupled TNTs to evoke Ca^{2+} liberation from the ER in the responding cell. A similar mechanism may pertain to gap junction-coupled cells that are directly abutting (e.g. endothelial cells; [27]) if the connexins channels represent a substantial barrier to buffered diffusion of Ca^{2+}. That is to say, although Ca^{2+} is the ‘message’, IP_3 is the ‘messenger’.

Supplementary Material

Refer to Web version on PubMed Central for supplementary material.

Acknowledgments

The authors thank Hiroshi Ohno (Riken Institute) for the HeLa-M-Sec cell line, David Spray (Albert Einstein College of Medicine) for the Cx43-sfGFP construct, and Brett Settle (University California Irvine) for developing the algorithm to control the UV laser spot system. This work was supported by National Institutes of Health grants GM 100201 to I.F.S, and GM 048071 and GM 065830 to I.P.

References

1. Rustom A, Saffrich R, Markovic I, Walther P, Gerdes HH. Nanotubular highways for intercellular organelle transport. Science. 2004; 303:1007–1010. [PubMed: 14963329]
2. Watkins SC, Salter RD. Functional connectivity between immune cells mediated by tunneling nanotubules. Immunity. 2005; 23:309–318. [PubMed: 16169503]
3. Hase K, Kimura S, Takatsu H, Ohmae M, Kawano S, Kitamura H, Ito M, Watarai H, Hazelett CC, Yeaman C, Ohno H. M-Sec promotes membrane nanotube formation by interacting with Ral and the exocyst complex. Nat Cell Biol. 2009; 11:1427–1432. [PubMed: 19935652]
4. Wittig D, Wang X, Walter C, Gerdes HH, Funk RH, Roehlecke C. Multi-level communication of human retinal pigment epithelial cells via tunneling nanotubes. PLoS One. 2012; 7:e33195. [PubMed: 22457742]
5. Smith IF, Shuai J, Parker I. Active generation and propagation of Ca2+ signals within tunneling membrane nanotubes. Biophys J. 2011; 100:L37–L39. [PubMed: 21504718]
6. Pasquier J, Galas L, Boulange-Lecomte C, Rioult D, Bultelle F, Magal P, Webb G, Le Foll F. Different modalities of intercellular membrane exchanges mediate cell-to-cell p-glycoprotein transfers in MCF-7 breast cancer cells. J Biol Chem. 2012; 287:7374–7387. [PubMed: 22228759]
7. Wang X, Bukoreshtliev NV, Gerdes HH. Developing neurons form transient nanotubes facilitating electrical coupling and calcium signaling with distant astrocytes. PLoS One. 2012; 7:e47429. [PubMed: 23071805]
8. He K, Shi X, Zhang X, Dang S, Ma X, Liu F, Xu M, Lv Z, Han D, Fang X, Zhang Y. Long-distance intercellular connectivity between cardiomyocytes and cardiofibroblasts mediated by membrane nanotubes. Cardiovascular research. 2011; 92:39–47. [PubMed: 21719573]
9. Sowinski S, Jolly C, Berninghausen O, Purbhoo MA, Chauveau A, Kohler K, Oddos S, Eissmann P, Brodsky FM, Hopkins C, Onfelt B, Sattentau Q, Davis DM. Membrane nanotubes physically connect T cells over long distances presenting a novel route for HIV-1 transmission. Nat Cell Biol. 2008; 10:211–219. [PubMed: 18193035]
10. Chinnery HR, Pearlman E, McMenamin PG. Cutting edge: Membrane nanotubes in vivo: a feature of MHC class II+ cells in the mouse cornea. J Immunol. 2008; 180:5779–5783. [PubMed: 18424694]
11. Osswald M, Jung E, Sahm F, Solecki G, Venkataramani V, Blaes J, Weil S, Horstmann H, Wiestler B, Syed M, Huang L, Ratliff M, Karimian Jazi K, Kurz FT, Schmenger T, Lemke D, Gommel M, Pauli M, Liao Y, Haring P, Pusch S, Herl V, Steinhauser C, Krunic D, Jarahian M, Miletic H, Berghoff AS, Griesbeck O, Kalamakis G, Garaschuk O, Preusser M, Weiss S, Liu H, Heiland S, Platten M, Huber PE, Kuner T, von Deimling A, Wick W, Winkler F. Brain tumour cells interconnect to a functional and resistant network. Nature. 2015; 528:93–98. [PubMed: 26536111]
12. Koyanagi M, Brandes RP, Haendeler J, Zeiher AM, Dimmeler S. Cell-to-cell connection of endothelial progenitor cells with cardiac myocytes by nanotubes: a novel mechanism for cell fate changes? Circulation research. 2005; 96:1039–1041. [PubMed: 15879310]
13. Onfelt B, Nedvetzki S, Benninger RK, Purbhoo MA, Sowinski S, Hume AN, Seabra MC, Neil MA, French PM, Davis DM. Structurally distinct membrane nanotubes between human macrophages support long-distance vesicular traffic or surfing of bacteria. J Immunol. 2006; 177:8476–8483. [PubMed: 17142745]
14. Xu W, Santini PA, Sullivan JS, He B, Shan M, Ball SC, Dyer WB, Ketas TJ, Chadburn A, Cohen-Gould L, Knowles DM, Chiu A, Sanders RW, Chen K, Cerutti A. HIV-1 evades virus-specific IgG2 and IgA responses by targeting systemic and intestinal B cells via long-range intercellular conduits. Nature immunology. 2009; 10:1008–1017. [PubMed: 19648924]

15. Gousset K, Schiff E, Langevin C, Marijanovic Z, Caputo A, Browman DT, Chenouard N, de Chaumont F, Martino A, Enninga J, Olivo-Marin JC, Mannel D, Zurzolo C. Prions hijack tunnelling nanotubes for intercellular spread. Nat Cell Biol. 2009; 11:328–336. [PubMed: 19198598]
16. Al Heialy S, Zeroual M, Farahnak S, McGovern T, Risse PA, Novali M, Lauzon AM, Roman HN, Martin JG. Nanotubes connect CD4+ T cells to airway smooth muscle cells: novel mechanism of T cell survival. J Immunol. 2015; 194:5626–5634. [PubMed: 25934863]
17. Wang X, Veruki ML, Bukoreshtliev NV, Hartveit E, Gerdes HH. Animal cells connected by nanotubes can be electrically coupled through interposed gap-junction channels. Proc Natl Acad Sci U S A. 2010; 107:17194–17199. [PubMed: 20855598]
18. Berridge MJ, Lipp P, Bootman MD. The versatility and universality of calcium signalling. Nat Rev Mol Cell Biol. 2000; 1:11–21. [PubMed: 11413485]
19. Paemeleire K, Martin PE, Coleman SL, Fogarty KE, Carrington WA, Leybaert L, Tuft RA, Evans WH, Sanderson MJ. Intercellular calcium waves in HeLa cells expressing GFP-labeled connexin 43, 32, or 26. Mol Biol Cell. 2000; 11:1815–1827. [PubMed: 10793154]
20. Bootman MD, Berridge MJ, Lipp P. Cooking with calcium: the recipes for composing global signals from elementary events. Cell. 1997; 91:367–373. [PubMed: 9363945]
21. Eugenin EA, Gaskill PJ, Berman JW. Tunneling nanotubes (TNT) are induced by HIV-infection of macrophages: a potential mechanism for intercellular HIV trafficking. Cellular immunology. 2009; 254:142–148. [PubMed: 18835599]
22. Demuro A, Parker I. "Optical patch-clamping": single-channel recording by imaging calcium flux through individual muscle acetylcholine receptor channels. J Gen Physiol. 2005; 126:179–192. [PubMed: 16103278]
23. Smith IF, Parker I. Imaging the quantal substructure of single inositol trisphosphate receptor channel activity during calcium puffs in intact mammalian cells. Proc Natl Acad Sci U S A. 2009; 106:6404–6409. [PubMed: 19332787]
24. Ellefson KS, Parker B, Smith I, IF. An algorithm for automated detection, localization and measurement of local calcium signals from camera-based imaging. Cell Calcium. 2014
25. Bejarano E, Yuste A, Patel B, Stout RF Jr, Spray DC, Cuervo AM. Connexins modulate autophagosome biogenesis. Nat Cell Biol. 2014; 16:401–414. [PubMed: 24705551]
26. Abounit S, Zurzolo C. Wiring through tunneling nanotubes--from electrical signals to organelle transfer. J Cell Sci. 2012; 125:1089–1098. [PubMed: 22399801]
27. Wilson C, Saunter CD, Girkin JM, McCarron JG. Clusters of specialized detector cells provide sensitive and high fidelity receptor signaling in the intact endothelium. FASEB journal : official publication of the Federation of American Societies for Experimental Biology. 2016; 30:2000–2013. [PubMed: 26873937]

Highlights

1. Nanotubes are long, thin membranous connections between distant cells.
2. Membrane nanotubes enable long-range Ca^{2+} signaling between distant cells.
3. Functional coupling through gap junctions is required for this to occur.
4. IP3 diffusion along the nanotube is responsible for Ca^{2+} signal propagation.
5. Ca^{2+} may be the ‘message’ but IP3 is the ‘messenger’!

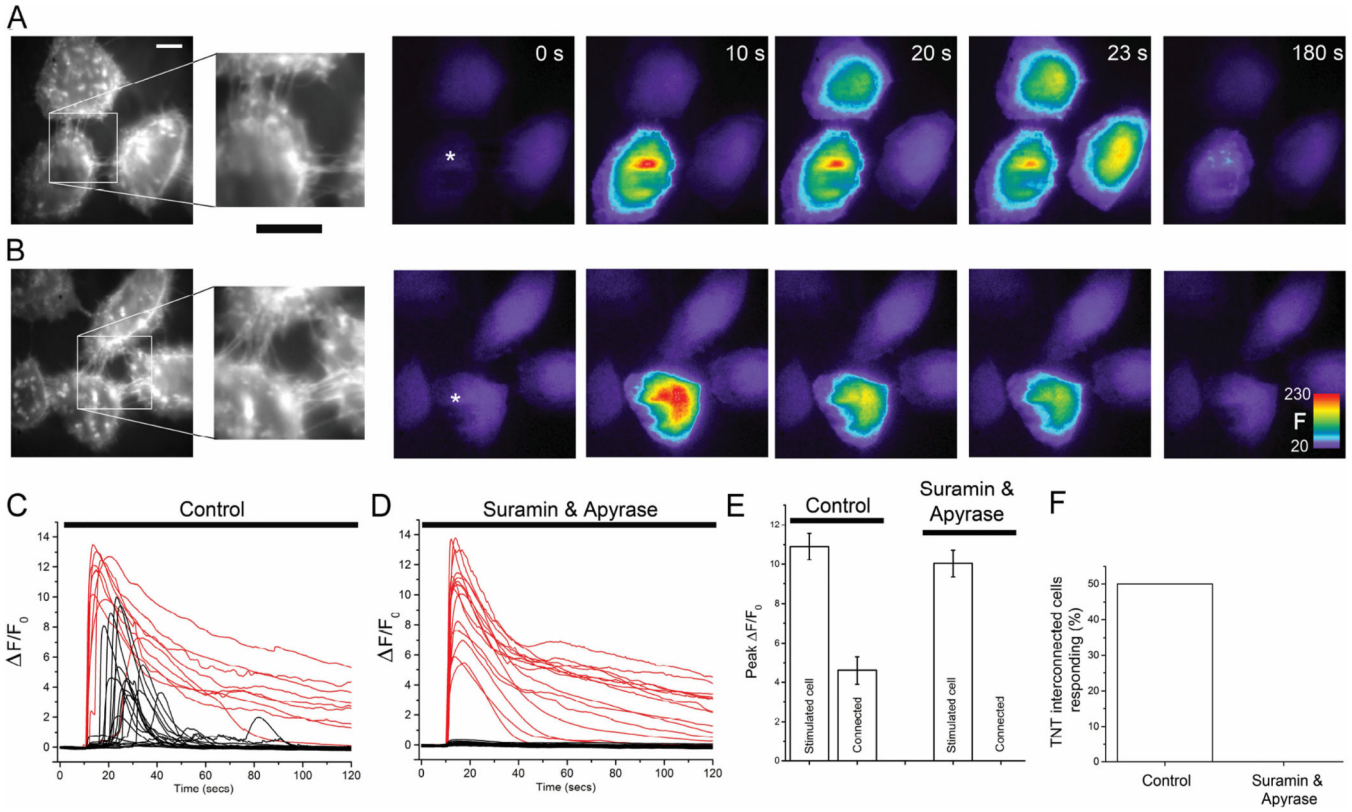

Fig. 1.

Transmission of Ca^{2+} signals between TNT-connected HeLa-M-Sec cells is abolished by blocking paracrine ATP signaling. (A, B) Monochrome panels at left show cells stained with Deep Red membrane marker to visualize cell membrane and TNTs. The insets show the regions of TNT connections at higher magnification. Scale bars = 10 μm. Subsequent color panels show Cal-520 fluorescence Ca^{2+} signals imaged in these cells at successive times following mechanical stimulation at 10 sec of a single cell (marked by asterisks). Warmer colors represent increasing Ca^{2+}-dependent fluorescence (F, arbitrary units). Responses were observed in TNT-connected surrounding cells in control conditions (A), whereas connected cells failed to respond in the presence of suramin and apyrase to block ATP-mediated signaling, even though the stimulated cell showed a robust response (B). (C) Traces showing Ca^{2+} fluorescence ratio signals ($\Delta F/F_0$) recorded from mechanically stimulated cells (red) and surrounding TNT-connected cells (black) in control conditions. Records are representative of experiments in which Ca^{2+} responses were observed in 17 out of 34 TNT-interconnected cells. (D) Corresponding, representative traces recorded in the presence of apyrase (20 units/ml) plus suramin (100 μM) to inhibit ATP-mediated signaling. (E) Mean peak amplitudes of Ca^{2+} signals ($\Delta F/F_0$) in mechanically stimulated cells and TNT-interconnected cells in control conditions and in the presence of suramin plus apyrase. (F) Percentages of TNT-interconnected cells responding to a cell that was mechanically stimulated. No Ca^{2+} responses were observed in surrounding TNT-connected (n = 28 cells) in the presence of apyrase and suramin.

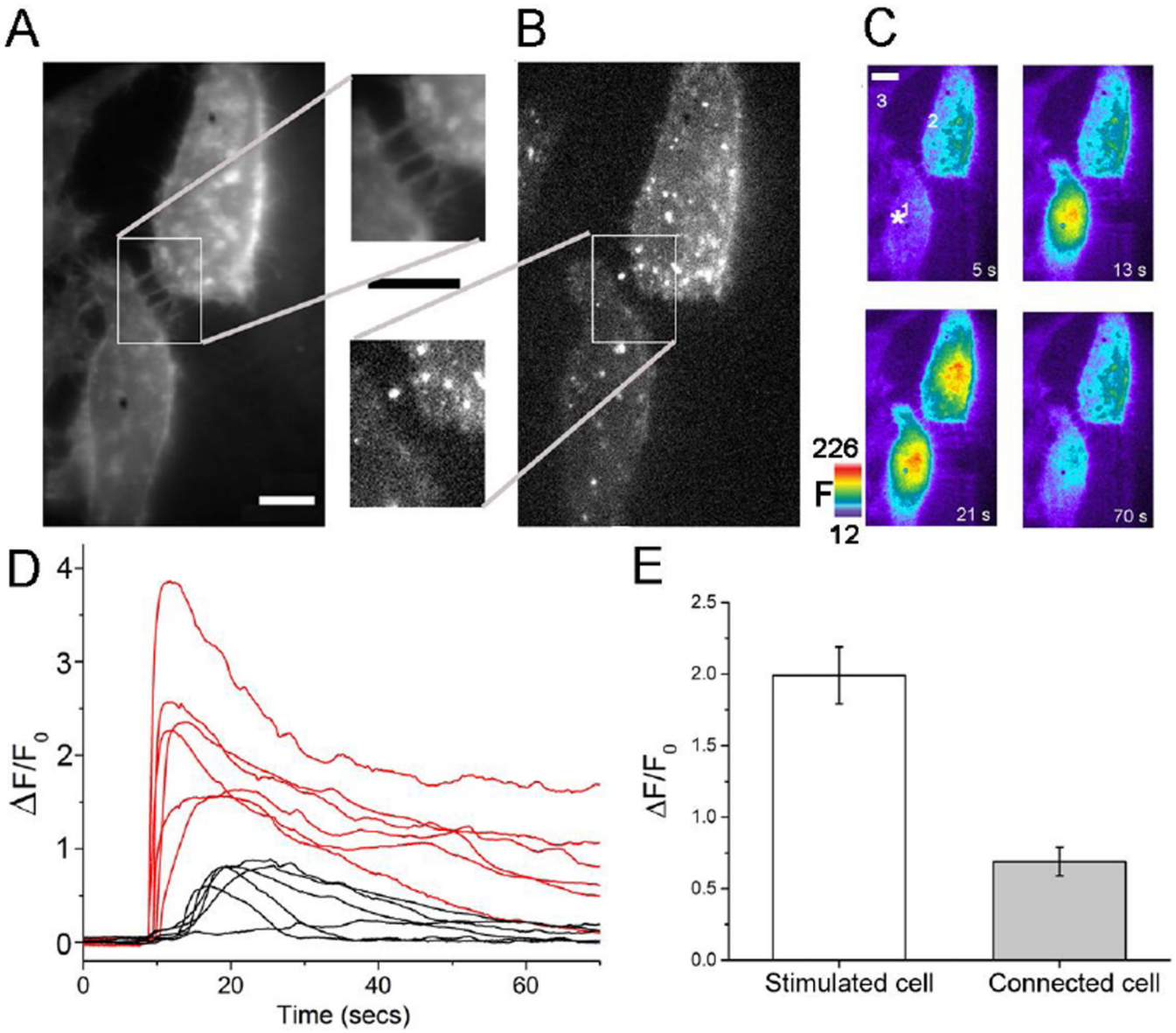

Fig. 2.

Expression of Cx43-sfGFP enables Ca^{2+} signal transmission between TNT-connected HeLa-M-Sec cells independent of paracrine ATP signaling. (A) Two TNT-connected HeLa-M-Sec cells visualized using Deep Red plasma membrane stain. The inset shows the region of TNT connections at higher magnification. Scale bars = 10 μm. (B) The same cells visualized by GFP fluorescence, demonstrating that both expressed Cx43-sfGFP. (C) Panels show Cal-590 Ca^{2+} fluorescence signals (F, arbitrary units) at different times before and after mechanical stimulation of one cell at t = 10s as indicated by the asterisk in the first panel. The TNT-connected cell (#2) showed a robust Ca^{2+} response after a delay (~ 7 s), whereas a neighboring Cx43-sfGFP-expressing but non-connected cell (#3) failed to respond. (D) Ca^{2+} fluorescence traces ($\Delta F/F_0$) from 6 trials in TNT-connected, Cx43-sfGFP-expressing cell pairs as in c, showing responses in stimulated cells (red) and corresponding responses in connected cells (black). (E) Mean peak amplitudes of Ca^{2+} fluorescence signals in

mechanically stimulated cells (open bar, n=13) and connected cells (grey bar) (n = 6). Fluorescence ratio changes ($\Delta F/F_0$) are smaller than in Fig 1. because resting fluorescence (F_0) was elevated by spectral bleed-through from the red membrane dye. All experiments were performed in the presence of apyrase (20 units/ml) and suramin (100 μM) to inhibit purinergic signaling.

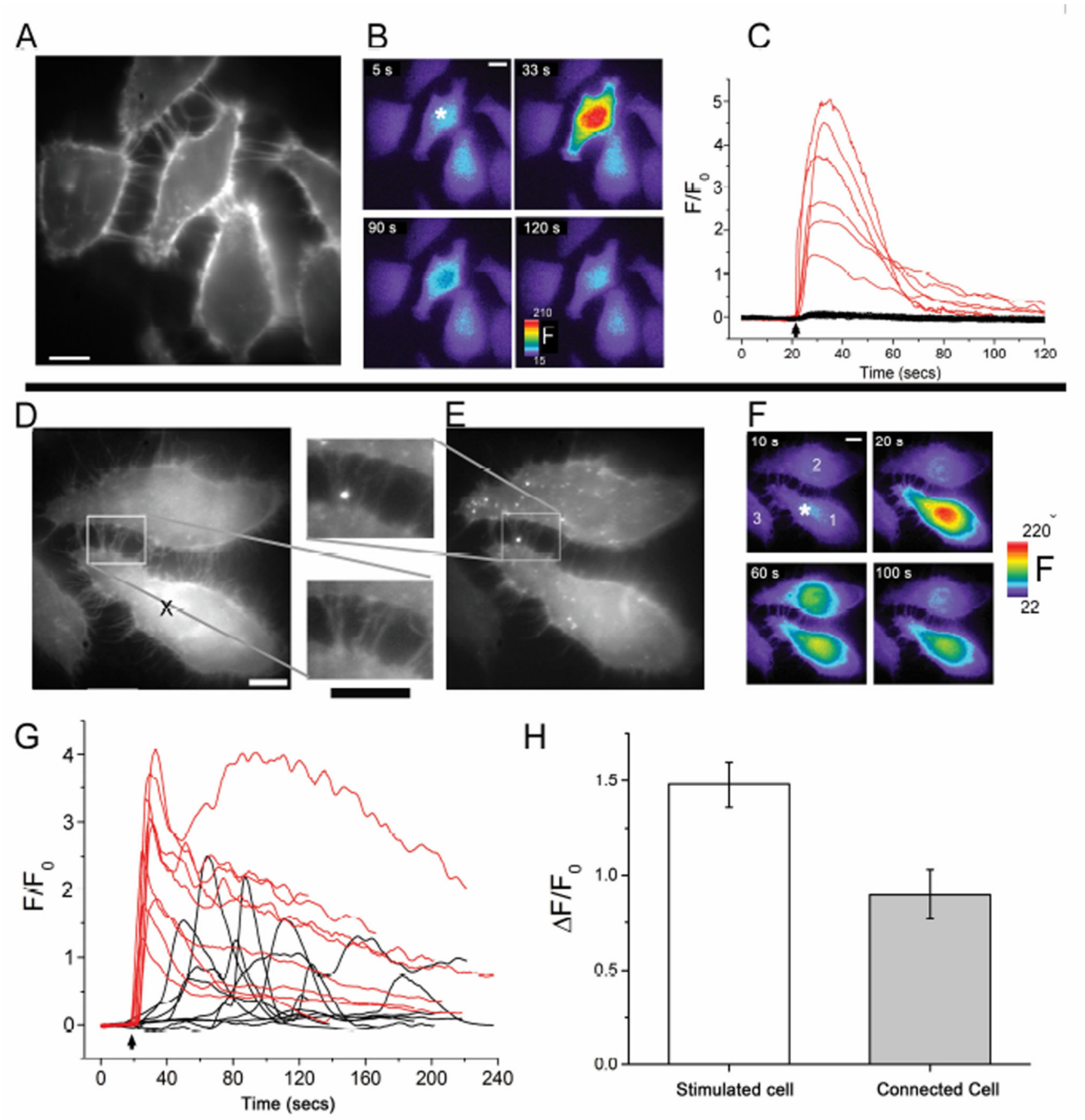

Fig. 3.

Transmission of Ca^{+} signals between TNT-connected Cx43-sfGFP-expressing cells following photorelease of ci-IP_3. (a-c), In naïve HeLa M-Sec cells (not expressing Cx43) local spot photorelease of i-IP_3 evokes robust Ca^{2+} signals in the stimulated cell, but not in surrounding, TNT-connected cells. (A) Field of cells stained with Deep Red membrane dye to visualize TNTs. Scale bar = 10 μm. (B) The same imaging field, showing Cal-520 Ca^{2+} fluorescence signals (F, arbitrary units) at different times before and after UV laser spot photolysis of caged i-IP_3 loaded into the cells. The laser spot (200 ms flash duration) was

delivered at t=21s, at the location marked with the asterisk in the first panel. (C) Traces show Ca^{2+} fluorescence signals ($\Delta F/F_0$) evoked in 6 cells stimulated by laser spot photorelease of i-IP_3 (red traces;, arrow indicates time of UV flash) and the lack of response in 16 surrounding, TNT-connected cells (black traces). (D-H) Expression of Cx43 in both cells of a TNT-connected pair enables communication of Ca^{2+} signals evoked by local photorelease of i-IP_3. (D, E), Images of a cell pair visualized using Deep Red membrane dye (D) and fluorescence of Cx43-sfGFP (E). Insets show magnified views of the TNT connection region. Scale bars = 10 μm. (F), The same imaging field, showing Cal-590 Ca^{2+} fluorescence signals (F, arbitrary units) at different times before and after UV laser spot photolysis of caged i-IP_3 loaded into the cells. The laser spot flash (~200 ms duration) was delivered at t=20s, at the location marked with the asterisk in the first panel. A second, TNT-connected, Cx43-expressing cell (cell #2) showed a Ca^{2+} response at a long (>35 s) latency following the response in the stimulated cell, while a third, TNT-connected but non-Cx43-expressing cell failed to respond (cell #3). (G) Traces showing Ca^{2+} fluorescence signals evoked in 9 cells directly stimulated by laser spot photorelease of i-IP_3 (red, arrow indicates time of UV flash) and responses in TNT-connected, Cx43-sfGFP expressing cells (black). (H) Mean peak amplitudes of fluorescence signals in 21 laser-spot stimulated cells (open bar) and in 9 responding, TNT-connected, Cx43-sfGFP expressing cells (grey bar).

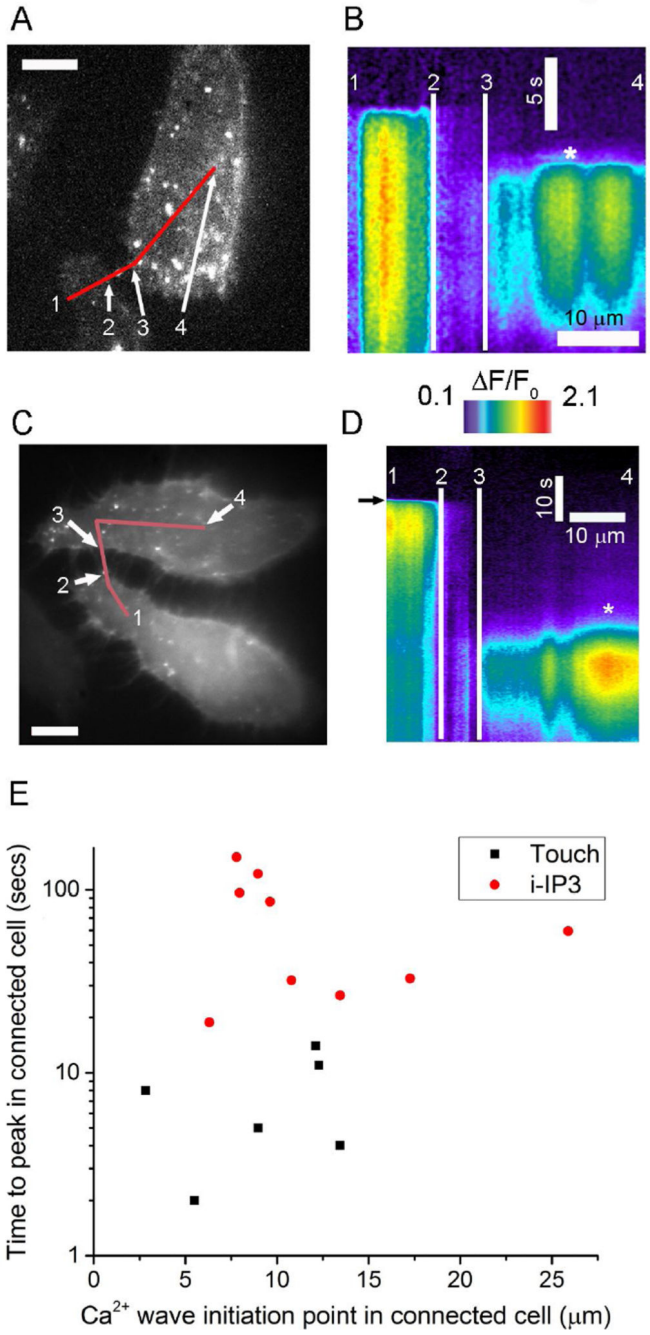

Fig. 4.

IP_3, and not Ca^{2+} itself, mediates transmission of Ca^{2+} signals via TNTs between Cx43 expressing cells. (A) Image showing fluorescence of Cx43-sfGFP in a pair of HeLa M-sec cells interconnected via TNTs (the same cells as in Fig. 2A). (B) Kymograph image (with time depicted vertically and distance horizontally) formed by measuring Ca^{2+} fluorescence changes ($\Delta F/F_0$) along the line marked in red in A as a function of time following mechanical stimulation of the lower cell. Notations (1,2,3,4) mark corresponding locations in the cell image and kymograph to delineate sites within each cell and the TNT connecting

them. The site of initiation of a Ca^{2+} signal in the connected cell is indicated by an asterisk. (C) Image showing fluorescence of Cx43-sfGFP in another pair of HeLa M-sec cells interconnected via TNTs (the same cells as in Fig. 3D). (D) Corresponding kymograph image where the lower cell was stimulated by spot photorelease of i-IP_3 when marked by the arrow. (E) Scatter plot showing distances from point of contact of TNTs to the site of initial Ca^{2+} response in the connected cell (x axis) and latency between peak times of Ca^{2+} signals in the stimulated and connected cells. Black squares are measurements with mechanical stimulation, and red circles are measurements with spot photorelease of i-IP_3. Time is depicted on a logarithmic axis to better encompass the wide spread in latencies observed between mechanical stimulation and photorelease of i-IP_3. All experiments involving mechanical stimulation were performed in the presence of apyrase (20 units/ml) and suramin (100 μM) to inhibit purinergic signaling.